

BI-DIRECTIONAL BEHAVIOR OF INTERIOR-, EXTERIOR-, AND CORNER-JOINTS OF RCS SYSTEM

Isao NISHIYAMA¹, Hiroshi KURAMOTO², Hidehiko ITADANI³ And Kunio SUGIHIRO⁴

SUMMARY

A composite and hybrid structural system, which is composed of reinforced concrete column and structural steel beam, provides many advantages over those employing conventional structural systems. In Japan, the potential usage of this structural system is the "shopping center" which requires long span with structural steel beam and high lateral stiffness by economical reinforced concrete column. So as to establish seismic design guidelines for this system, extensive analytical and experimental research was carried out under the U.S.-Japan Cooperative Earthquake Research Program on Composite and Hybrid Structures. However, the tentative guidelines completed in the Japanese side do not take into account the bi-directional behavior of the beam-to-column joints due to the lack of the technical data. Thus, six three-dimensional beam-to-column joints subjected to bi-directional seismic force were experimented. This paper presents the experimental result of the bi-directional behavior of the 3-D joints with various geometries such as interior column joint, exterior column joint, corner column joint and roof joint.

INTRODUCTION

A composite and hybrid structural system, which is composed of reinforced concrete column and structural steel beam (RCS), provides many advantages over those employing conventional systems. In Japan, the potential use of this structural system is the "shopping center" which requires long span with structural steel beam and high lateral stiffness by economical reinforced concrete column. While, structural engineers in the U.S. are very much interested in the quick construction sequence of this system using small erection structural steel column which is applicable to medium- to high-rise office buildings (Iyengar 1984). Some private construction companies in Japan developed their own design method for this structural system (Tominaga et al. 1986; Yoshino et al. 1987). However, they are not a generalized design method and their scope of application is quite limited. The ASCE guidelines ("Guidelines" 1994) give practical design method for this system, but it is only applicable to interior beam-to-column joints. So as to establish generalized (common) seismic design method both for Japan and for the U.S., this structural system was selected as one of the target structural systems to be studied under the U.S.-Japan Cooperative Earthquake Research Program on Composite and Hybrid Structures ("Recommendations" 1992) from 1993 fiscal. A large number of experimental and macro / micro model analytical study have been carried out up to now on the beam-to-column joints subjected to seismic force in the direction of their principle axis, which in most cases resulted in ductile behavior. However, bi-directional seismic response of the three dimensional (3-D) beam-to-column joints has never been studied yet. Therefore, the influence of bi-directional loading interaction on the stiffness, strength and ductility of the beam-to-column joints was experimentally studied by six specimens with interior, exterior, corner and roof joint details.

¹ Building Research Institute (BRI), Ministry of Construction, Japan. E-mail: isao@kenken.go.jp

² Head, Aero-dynamics Division, Structural Engineering Department, BRI. E-mail: kura@kenken.go.jp

³ OHOMOTO-GUMI Co., Nagata 2-17-3, Chiyoda-ku, Tokyo 100-0014, Japan. Email: itadani@gw.ohmoto.co.jp

⁴ Iguchi-Suzugadai 3-15-18-102, Nishi-ku, Hiroshima 733-0843, Japan. E-mail: dog@d3.dion.ne.jp

DESCRIPTION OF TEST SPECIMENS

Six through column joint specimens (BRI-8, BRI-9, BRI-10, BRI-12, BRI-13 and BRI-14) were constructed. In Figure 1, the plan and the elevation of the interior column joint specimen (BRI-8) are shown as an example. The joint details are also shown in Figure 1. The dimensions of the specimens are summarized in Table 1. The mechanical properties of structural steel, reinforcing bar and concrete are also in Table 1.

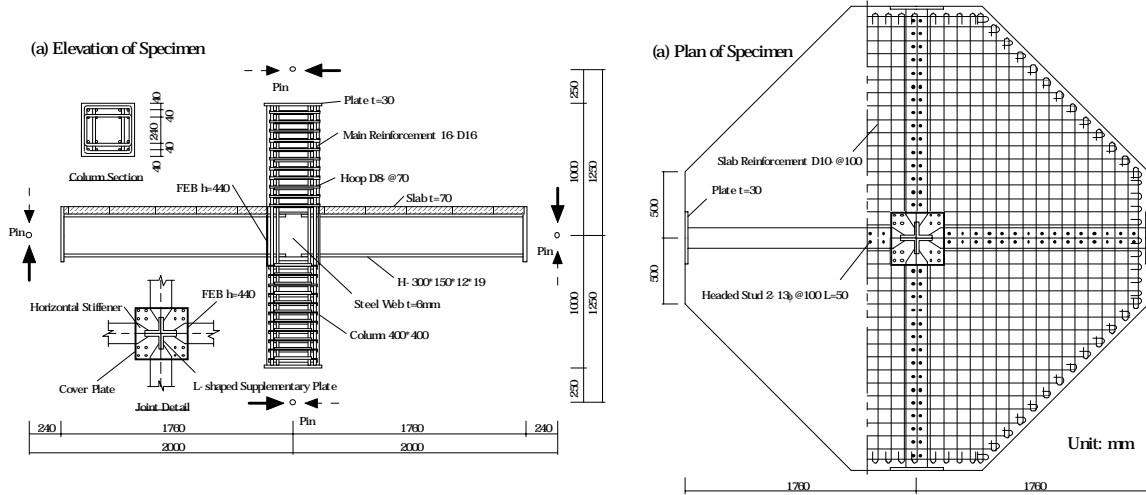


Figure 1: Specimen shape and details of beam-to-column joints

Table 1: Dimensions of specimens and mechanical properties of materials

Specimen	BRI- 8	BRI- 9	BRI- 10	BRI- 12	BRI- 13	BRI- 14	
Geometry & Loading 							
Span * Height	4000 mm * 2500 mm						
Column	Section	400 mm * 400 mm					
	Main rebar	16 D16 ($\sigma_y=472\text{MPa}$ $\sigma_t=665\text{MPa}$)			16 D16 ($\sigma_y=555\text{MPa}$ $\sigma_t= 677\text{MPa}$)		
	Hoop	4 D8@70 ($\sigma_y=916\text{MPa}$ $\sigma_t=1073\text{MPa}$)			4 D8@70 ($\sigma_y=1034\text{MPa}$ $\sigma_t= 1110\text{MPa}$)		
	Concrete	F _c =29MPa (lower column) & F _c =26MPa (upper column)			F _c =28MPa (lower column) & F _c =27MPa (upper column)		
Beam	Section	BH- 300* 150* 12* 19					
Panel	Steel web	t=6mm ($\sigma_y=305\text{MPa}$ $\sigma_t=413\text{MPa}$)			t=6mm ($\sigma_y=347\text{MPa}$ $\sigma_t=456\text{MPa}$)		
	Horizontal stiffener	t=19mm ($\sigma_y=363\text{MPa}$ $\sigma_t=527\text{MPa}$)			t=19mm ($\sigma_y=373\text{MPa}$ $\sigma_t=533\text{MPa}$)		
	Cover plate	t=6mm ($\sigma_y=305\text{MPa}$ $\sigma_t=413\text{MPa}$)			t=6mm ($\sigma_y=347\text{MPa}$ $\sigma_t=456\text{MPa}$)		
	FBP	t=12mm ($\sigma_y=264\text{MPa}$ $\sigma_t=428\text{MPa}$)			t=12mm ($\sigma_y=286\text{MPa}$ $\sigma_t=440\text{MPa}$)		
RC slab	t=70mm D10@100 ($\sigma_y=349\text{MPa}$ $\sigma_t=497\text{MPa}$)						
Column axial force	931kN (0.2N _o) : constant			max : 1411kN (0.3N _o) min : 0kN	max : 1882kN (0.4N _o) min : - 118kN (-.025N _o)	0 kN : constant	

σ_y = yield strength, σ_t =tensile strength

The reinforced concrete column, which is common to all specimens, is 2.5m in height and is 400mm both in depth and width. As BRI-14 is the roof joint, it does not have upper column. The structural steel beam is a welded H-section with 300mm in depth, 150mm in flange width, 19mm in flange thickness and 12mm in web thickness. The steel beam and the reinforced concrete slab (t=70mm) are connected with headed studs to work as a composite beam. Casting concrete was done with vertical position. Lower column including floor slab was cast first and then upper column was cast.

The panel-zone is comprised of steel web ($t=6\text{mm}$) panel, concrete panel, triangular shaped horizontal stiffener ($t=19\text{mm}$), face bearing plate (FBP; $t=12\text{mm}$) extended 70mm above and below the beam flanges, cover plate ($t=6\text{mm}$), L-shaped supplementary plate ($t=12\text{mm}$) and main reinforcing bars (16-D16) which run vertically through the panel-zone. As the beam flanges were transformed into triangular plates (stiffeners) in the panel-zone, this joint detail is called through column type.

The dimensions and the details of the specimens were so decided that the test results of interior column joints can be easily compared with those from the 2-D similar previous tests (Kuramoto 1996). The objectives of this experimental study is to make clear the bi-directional inelastic behavior of beam-to-column joints. Therefore, the specimens of interior column joints were designed to fail in shear at panel-zone. Thus, the plate thickness of the steel web panel was chosen as half of that of the beam web. The composite beam was designed strong enough not to fail prior to the panel-zone. Number of main reinforcing bars and their size were determined to increase the column resistance to bond splitting failure and the flexural yield over the expected shear strength of the panel-zone. Other specimens with different geometries were for comparison with interior column joints, so the joint details were kept as the same.

TEST SETUP AND LOADING PROCEDURE

Setup of a loading apparatus is shown in Figure 2. Column bottom is free to rotate about x- and y-axis, but is restraint its rotation about z-axis. Four actuators (No.5, No.6, No.7 and No.8) are pin connected to the loading block at the column top. The actuators of No.5 and No.6 restrain the column top from the rotational displacement about z-axis and the translational displacement to the direction of y-axis. Actuator No.7 restrains the translational displacement to the direction of x-axis. Actuator No.8 gives column axial force. The simulated bi-directional seismic force is applied by four displacement controlled actuators attached to each free end of the steel beam (No.1, No.2, No.3 and No.4). Column shear force is estimated from the reaction force in the actuators of No.5, No.6 and No.7.

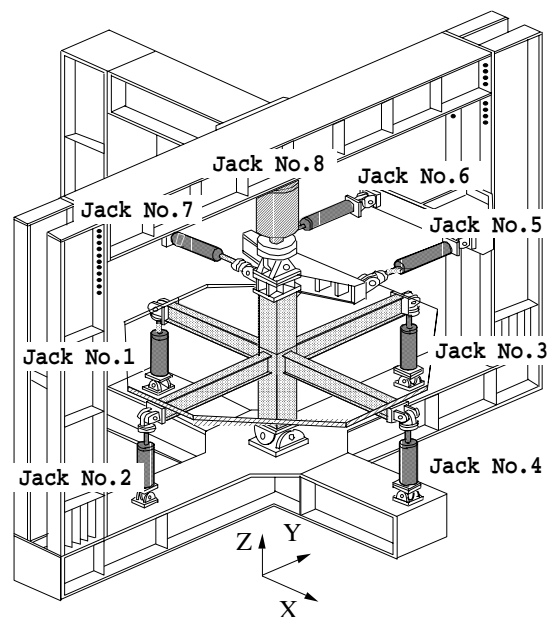


Figure 2: Test setup

In case of interior column joint specimens (BRI-8, BRI-9 and BRI-10), the column compressive force (gravity load) was kept constant as 931kN (95tonf), which corresponds to about 20% of the column compressive strength. In case of exterior column joint specimen (BRI-12), the column compressive force was varied between zero and 1411kN (144tonf) considering overturning effect. Gravity load of 706kN (72tonf) corresponds to about 15% of the column compressive strength, and the overturning force corresponds to plus / minus 706kN (72tonf). In this specimen, displacement controlled actuator No.2 was not necessary to be used. In case of corner column joint specimen (BRI-13), the column compressive force was planned to vary between -941kN (-96tonf) and 1882kN (192tonf) considering overturning effect. Gravity load of 470kN (48tonf) corresponds to about 10% of the column compressive strength, and the overturning force corresponds to plus / minus 1411kN (144tonf). Due

to the inappropriate anchorage of the main reinforcing bars at the end of the column, the column tensile force was limited to -118kN (-12tonf). In this specimen, both No.1 and No.2 actuators were not necessary to be used.

In case of roof joint specimen (BRI-14), the actuators No.2, No.5, No.6, No.7 and No.8 in Figure 2 were not used, which resulted in instability of the specimen. Instead, the x-directional displacement at free end of the steel beam No.1 and the y-directional displacement of steel beam No.3 were restrained to stabilize the specimen as shown in Figure 3. Overall torsional deflection of the specimen was not restraint specially, but the observed torsional deflection was negligible. The column reinforcing bars simply stick out the roof floor slab without special anchorage.

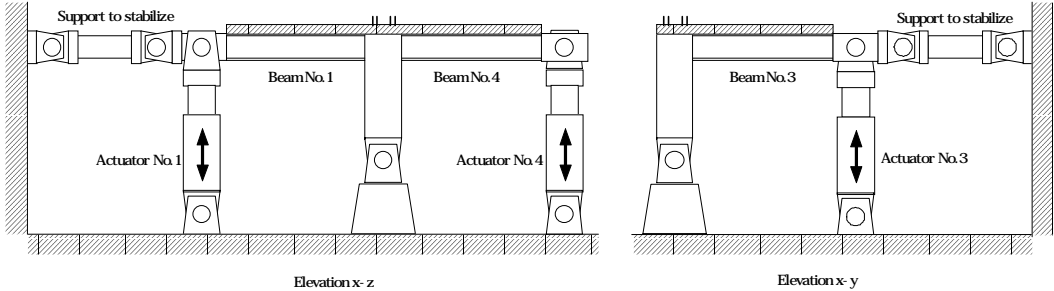


Figure 3: Actuator arrangement to stabilize roof joint specimen

The typical loading patterns are shown in Figure 4. The amplitude of the story drift angle in the reversed cyclic loading is increased such as 0.25%, 0.5%, 1%, 1.5%, 2%, 3%, 4% and 5%. Smaller displacement amplitudes are added after larger ones to see the damping characteristics of the beam-to-column joints. Uni-directional loading pattern was adopted in BRI-8, in which the loading direction was coincided with the principle axis (y-axis) of the specimen. In BRI-9, the direction of the uni-directional loading was set at 45 degrees with respect to its principle axis. Other specimens such as BRI-10, BRI-12, BRI-13 and BRI-14 were loaded in both principle directions simultaneously forming a circular orbit. The circle load pattern starts from y-directional positive loading up to the prescribed displacement amplitude. Then, one or two cycles of circle loading to the clockwise direction follows. Finally, uni-directional reversed loading in the direction of principle axis (y-axis) starting from unloading follows. This load sequence was repeated by increasing the displacement amplitude.

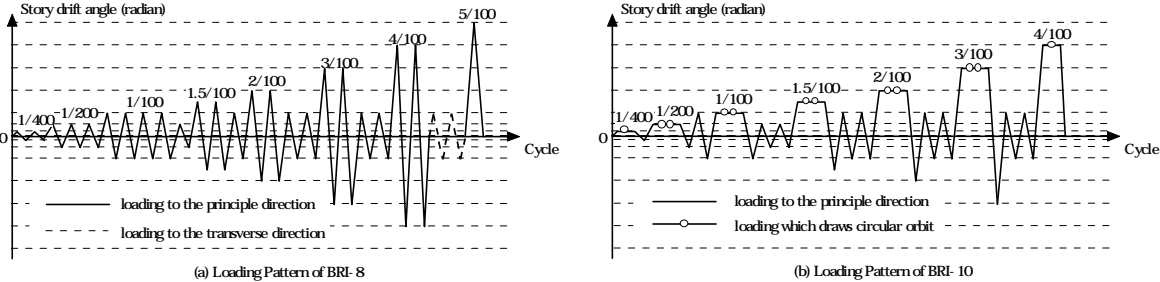


Figure 4: Typical loading patterns

SPECIMEN BEHAVIOR AND TEST RESULTS

The test results are summarized in Table 2. Column shear force versus story drift angle relationships are shown in Figure 5, where column shear force and story drift angle are estimated as the components in the loading direction in case for BRI-8 and BRI-9, and are estimated as the components of the y-direction in case for other specimens loaded in both principle directions forming a circular orbit. Figure 6 shows the equivalent viscous damping of BRI-8 and BRI-10.

Table 2: Test results

Specimen	*1 Q _{max} (tonf)	Drift angle at Q _{max} (%)	Failure mode	Calculated strength (tonf)	
				*2 Panel shear	*3 Column Flexural
BRI- 8	33.3	4	Shear yield in panel- zone	21.8	y- direction 31.8
BRI- 9	33.4	4	Shear yield in panel- zone and flexural yield in column		45deg- direction 27.6
BRI- 10	29.0	3	Shear yield in panel- zone followed by spalling of cover concrete		
BRI- 12	33.7	3	Shear yield in panel- zone and flexural yield in column	22.9	y- direction 37.4
BRI- 13	32.5	3	Shear yield in panel- zone and flexural yield in column		45deg- direction 32.5
BRI- 14	29.6	3	Slippage of column main reinforcement		

*1 Experimental maximum strength

*2 The maximum strength is estimated as 1.1 times of the strength given by JCI proposed formula ("Report of Composite Structure Research Committee" (1991), Japan Concrete Institute) based on the result of the previous test (Kuranoto 1996).

*3 Flexural strength of column is estimated by section analysis, in which the strength is determined at the tensile yield of all tension side reinforcing bars.

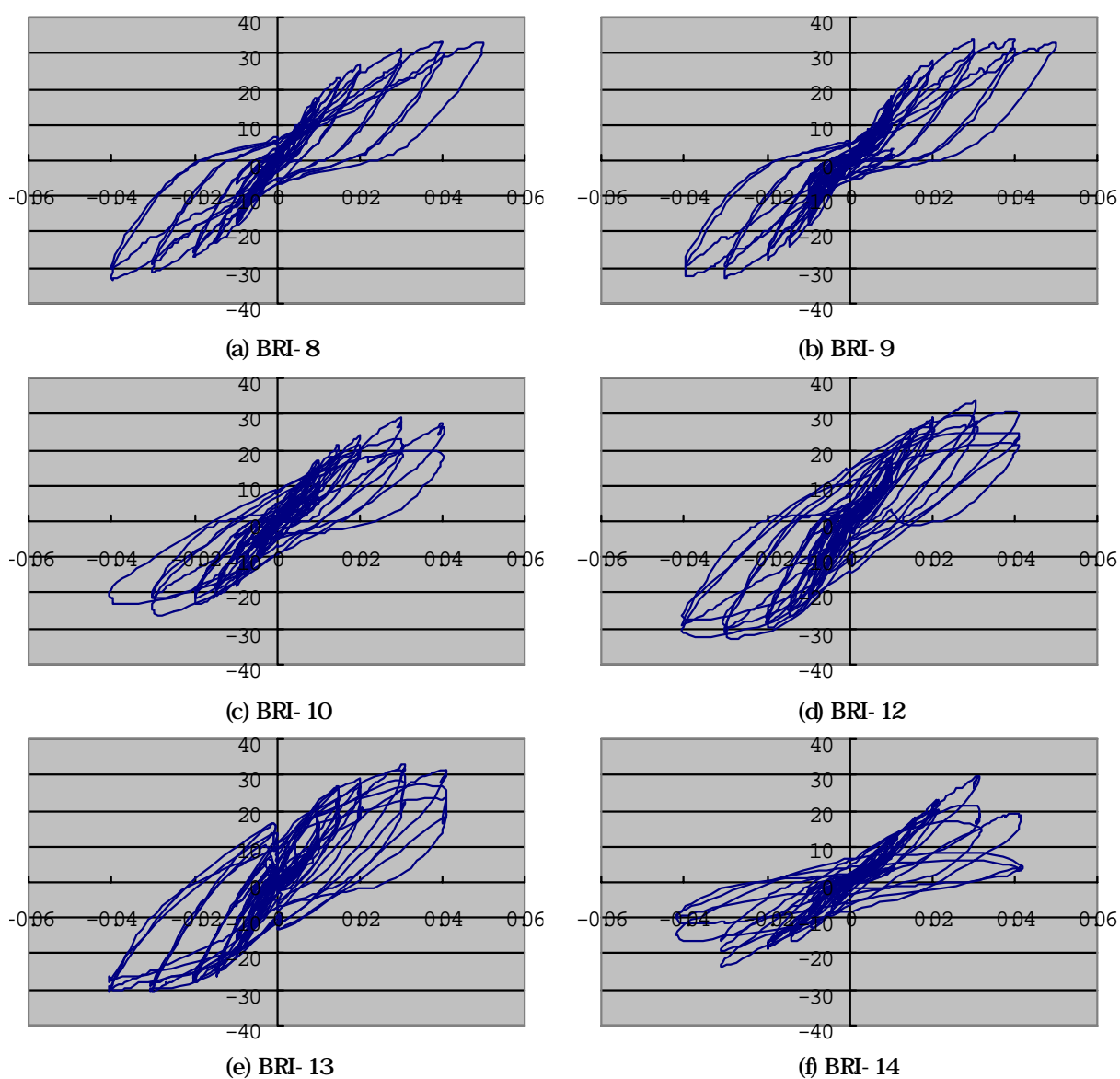


Figure 5: Column shear force versus story drift angle (tonf vs. radian)

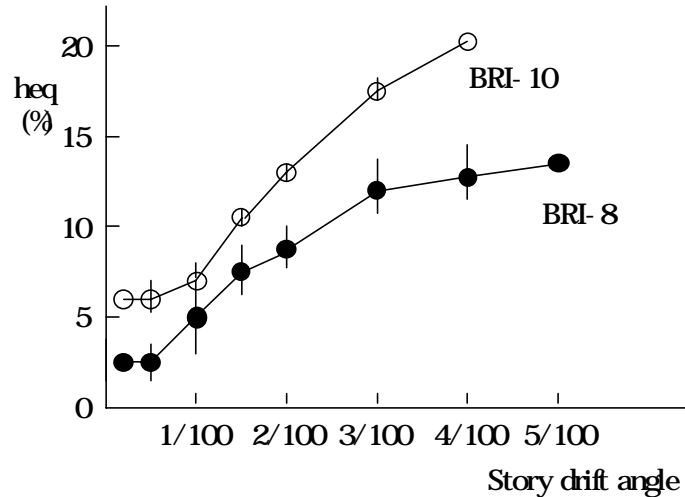


Figure 6: Equivalent viscous damping of BRI-8 and BRI-10

Effect of Loading Direction

The effect of loading direction is discussed by comparing the initiation of column flexural crack, the shear yield of the steel web panel, the tensile yield of plates and reinforcing bars, and the hysteresis loops of the specimens of BRI-8, BRI-9 and BRI-10. Due to the limited pages of manuscript, some of the figures are not presented. But the general conclusions are; 1) The effect of loading direction appeared to be not effective to overall hysteresis behavior (BRI-8 vs. BRI-9). 2) The influence of bi-directional loading drawing circular orbit was quite large especially in the hysteresis loop. In the circular orbit loading, the shape of the hysteresis loop changed from pinched to spindle-shaped, and the maximum strength reduced by 10% (BRI-8 vs. BRI-10).

General behavior

Column flexural crack occurred at the story drift angle of 0.5% in case for BRI-8. Then, shear yield of the steel web panel followed at the story drift angle of 1%. Tensile yield of the L-shaped supplementary plates was observed at 1.5% drift and the tensile yield in main reinforcing bar was observed at 3% drift. The maximum column shear strength of 326kN (33.3tonf) was reached at the story drift angle of 4%. The hysteresis loop was a little pinched but the ductility was fairly large. The equivalent viscous damping estimated in each half cycles increases as the displacement amplitude increases, and it reached about 13% in the final stage as shown in Figure 6. The tensile strain on the steel web panel reached 1%, while that on the main reinforcing bar stayed within elastic range.

As for BRI-9, column flexural crack initiated at the story drift angle of 0.5%. Then, shear yield of the steel web panel followed at 1% drift. Tensile yield of both the L-shaped supplementary plate and the main reinforcing bar was observed at 2% drift. The maximum column shear strength reached 327kN (33.4tonf), which well agreed with that of BRI-8, at the story drift angle of 4%. Although the hysteresis loop of BRI-9 was a little more pinched than that of BRI-8, they look quite similar to each other up to the story drift angle of 4%, after which there was a clear reduction in strength in BRI-9. The tensile strain on the steel web panel was about a half of that of BRI-8. The tensile strain of the main reinforcing bar reached to about 1%.

As for BRI-10, column flexural crack occurred at the story drift angle of 1% in the first loading cycle. In the subsequent loading cycle of the same displacement amplitude, yielding of the steel web panel and the L-shaped supplementary plate was detected, which is somewhat earlier than BRI-8 and BRI-9. The maximum column shear strength of 284kN (29.0tonf) in the direction of y-axis and 251kN (25.6tonf) in the direction of x-axis were reached at the story drift angle of 3%. The maximum strength is about 10% less than those of the specimens loaded uni-directionally. The hysteresis loop looks quite different from those of BRI-8 and BRI-9, and it follows elliptic curve. Looking the hysteresis loop more closely, the restoring force characteristics in the first principle directional loading are similar to those of BRI-8 and BRI-9 with slightly pinched behavior, but those in the subsequent cycles of the circle load pattern shows spindle shape and the strength gradually reduced as the cycle

of the circular load pattern increases even within the small displacement amplitude. The tensile strain on the steel web panel reached 0.8% and that of the main reinforcing bar is at most yield strain.

Maximum strength

The maximum column shear strength loaded in the principle direction (BRI-8) well agreed with that loaded at 45 degrees with respect to the principle direction of the specimen (BRI-9), which clearly shows the insensitivity of the loading direction on the strength. The shear strengths of these specimens are about 50% greater than the calculated one based on the previous similar test result (Kuramoto 1996). The reason of this large discrepancy seems to relate with the existence of the L-shaped supplementary plates, which are placed to prevent local yielding in the beam web panel in the early stage of loading. The maximum strength of the specimen loaded by a circular load pattern (BRI-10) was 10% less compared to those of BRI-8 and BRI-9.

Effect of Joint Geometry

The effect of joint geometry is discussed by comparing the hysteresis loops and the maximum strengths of BRI-12, BRI-13, BRI-14 and BRI-10. The conclusions obtained can be simply summarized as follows; 1) The effect of joint geometry appeared to be not effective to overall hysteresis behavior. 2) It affects little on the maximum strength of the joints. Exterior column joint and corner column joint strengths did not fall below that of the interior column joint (BRI-12, BRI-13 vs. BRI-10). 3) Roof joint behavior is significantly affected by the slippage of the anchorage of the main reinforcing bar.

General behavior

The hysteresis loops of beam-to-column joints, which subjected to bi-directional loading drawing a circular orbit, are shown in Figure 5. Only the roof joint specimen (BRI-14) showed unstable hysteresis loop due to the anchorage failure of the column reinforcement at the top of the floor slab. The other three joints showed stable spindle shaped hysteresis loops. If the loops of BRI-13, BRI-12 and BRI-10 are compared, it can be seen as the tendency that the less beam joint shows better behavior than others (BRI-13 > BRI-12 > BRI-10). The reason will be the issue in the future.

Maximum strength

The maximum strength of BRI-12 was 330kN (33.7tonf), and that of BRI-13 was 319kN (32.5tonf), while that of BRI-114 was 290kN (29.6tonf). The joint details are the identical in these specimens. As the joint subjects to the confinement by the adjacent beams, it is anticipated that the joint, which has less number of beams, shows less strength. However, test result showed inversely, that is, the strength of four beam joint (BRI-10) was about 10-15% less compared to three beam joint (BRI-12) and two beam joints (BRI-13). Meanwhile, the strength of roof joint (BRI-14) was terminated by the failure of the anchorage of column main reinforcements. As seen in Figure 3, it will be indicated the importance of anchorage of the reinforcement at the roof joint.

CONCLUSIONS

In total, six three-dimensional joint experiments were completed. Three of them were interior column joints; one of them was loaded in the direction of the beam (principle axis), the next one was loaded in the direction of 45 degrees with respect to the principle axis, the last one was loaded simultaneously in the direction of the principle axis and its perpendicular direction drawing circular loading orbit (bi-directional loading). One exterior column joint specimen was bi-directionally loaded with varying column axial thrust simulating overturning effect. One corner column joint specimen was also loaded bi-directionally. The roof joint was also loaded bi-directionally but with column zero axial thrust. The strength and ductility including hysteresis characteristics of the six specimens were presented. And, the effect of loading direction, bi-directional loading and joint geometries were discussed. The following conclusions were obtained from the comparison of the test results: 1) The effect of loading direction appeared to be not effective to overall hysteresis behavior (BRI-8 vs. BRI-9). 2) The influence of bi-directional loading drawing circular orbit was quite large especially in the hysteresis loop. In the circular orbit loading, the shape of the hysteresis loop changed from pinched to spindle-shaped, and the maximum strength reduced by 10% (BRI-8 vs. BRI-10). 3) The effect of joint geometry appeared to be not effective to overall hysteresis behavior. Exterior column joint and corner column joint did not fall below that of the interior

column joint (BRI-12, BRI-13 vs. BRI-10). 4) Roof joint behavior is significantly affected by the slippage of the anchorage of the main reinforcing bar.

This paper presented the test results of the beam-to-column joints with various geometries, which have the identical joint details (reinforcements). Therefore, the obtained conclusions are only applicable to the adopted joint details and further study on other joint details are in need.

ACKNOWLEDGEMENT

The writers wish to express their gratitude to the members of the Joint Technical Coordinating Committee of the U.S.-Japan Cooperative Earthquake Research on Composite and Hybrid Structures (Co-chairman: Profs. H. Aoyama and S. Mahin), who encouraged the writers and cordially gave advice. The writers are also grateful to Prof. H. Noguchi for his suggestion and discussion as the chairman of the Technical Sub-Committee on RCS system.

REFERENCES

"Guidelines for Design of Joints between Steel Beams and Reinforced Concrete Columns." (1988). ASCE Task Committee on Design Criteria for Composite Structures in Steel and Concrete, J. Struct. Engrg., ASCE, 120(8), 2330-2357.

Iyengar, H.(1984). "Recent Developments in Mixed Steel-Concrete Systems." ASCE, Composite and Mixed Construction edited by C.W. Roeder, December, 173-184.

Kuramoto, H. (1996). "Seismic Resistance of Through Column Type Connections for Composite RCS Systems." Eleventh World Conference on Earthquake Engineering, Acapulco, Mexico, June 23-28.

"Recommendations for U.S.-Japan Cooperative Research Program - Phase 5 Composite and Hybrid Structures." (1992). Edited by Goel S. and Yamanouchi H., Report No.UMCEE 92-29, University of Michigan, Ann Arbor, MI.

Tominaga, H. et al. (1986). "Strength and Ductility of Frames Composed of RC Columns and Steel Beams (Part 1)." Architectural Institute of Japan, Summaries of Technical Papers of Annual Meeting, C, 1427-1428 (in Japanese).

Yoshino T. et al. (1987). "Experimental Study on Composite Structure of Reinforced Concrete Column-Steel Beam (Part 1)." Architectural Institute of Japan, Summaries of Technical Papers of Annual Meeting, C, 1315-1316 (in Japanese).